

Dalton Transactions

Accepted Manuscript



This is an *Accepted Manuscript*, which has been through the RSC Publishing peer review process and has been accepted for publication.

Accepted Manuscripts are published online shortly after acceptance, which is prior to technical editing, formatting and proof reading. This free service from RSC Publishing allows authors to make their results available to the community, in citable form, before publication of the edited article. This *Accepted Manuscript* will be replaced by the edited and formatted *Advance Article* as soon as this is available.

To cite this manuscript please use its permanent Digital Object Identifier (DOI®), which is identical for all formats of publication.

More information about *Accepted Manuscripts* can be found in the [Information for Authors](#).

Please note that technical editing may introduce minor changes to the text and/or graphics contained in the manuscript submitted by the author(s) which may alter content, and that the standard [Terms & Conditions](#) and the [ethical guidelines](#) that apply to the journal are still applicable. In no event shall the RSC be held responsible for any errors or omissions in these *Accepted Manuscript* manuscripts or any consequences arising from the use of any information contained in them.

Cite this: DOI: 10.1039/c0xx00000x

www.rsc.org/xxxxxx

PAPER

Interaction of oxovanadium(IV)–salphen complexes with bovine serum albumin and their cytotoxicity against cancer

Velusamy Gomathi Sankareswari^a, Devaraj Vinod^b, Ayyasamy Mahalakshmi^c, Meena Alamelu^d Ganesan Kumaresan^d, Ramasamy Ramaraj^{a*} and Seenivasan Rajagopal^{a*}

⁵ Received (in XXX, XXX) Xth XXXXXXXXXX 20XX, Accepted Xth XXXXXXXXXX 20XX

DOI: 10.1039/b000000x

Vanadyl compounds of clinical significance are recommended as drugs against diseases such as tuberculosis, diabetes, cancer, etc. In order to check the potential of the salphen ligands and oxovanadium(IV)–salphen complexes as drugs their binding with bovine serum albumin (BSA) is investigated. The binding constants measured at pH 7.4 using UV–vis absorption and fluorescence techniques are in the range of 10^3 – 10^5 M⁻¹. The quenching of the fluorescence of BSA and appearance of enhanced luminescence of salphen ligand/vanadium(IV) complex at the increased [quencher] shows efficient FRET from the protein to the quencher and the distance of energy transfer estimated using Forster theory is in the range of 1.4 – 3.5 nm. Molecular docking studies utilizing (DFT) oxovanadium(IV)–salphen derivatives show strong binding with BSA and give in-sight of the binding modes, interaction pattern and stability of synthesized complexes in the target site. The cytotoxicity study shows the ability of these V(IV) complexes to inhibit the growth of AGS gastric cell lines.

Introduction

Vanadium, a transition metal abundant (~0.02%) in nature, exists under physiological conditions predominantly in the anionic vanadate, HVO_4^{2-} , form (oxidation state +5) or as the vanadyl (+4) cation (VO^{2+})¹ though oligomeric and protonated V(V) species (H_2VO_4^-) are possible depending on the pH and concentration. The anionic form resembles phosphate to some extent, while the vanadyl cation to Mg^{2+} .² The use of vanadium in humans is recommended in cases of pathological states such as malnutrition, anemia, tuberculosis and diabetes.³ Vanadyl (VO^{2+}) compounds are less toxic than vanadates. Vanadyl compounds with different coordination modes have been designed and synthesized for their clinical use.^{4,5} Some Schiff–base complexes of oxovanadium(IV) display insulin–enhancing properties when administered as therapeutic agents.⁶ In particular Schiff–base complexes of oxovanadium(IV) with the N_2O_2 chromospheres have been shown to normalize blood glucose level with high efficiency, even at low concentration, with low toxicity.⁷ Serum albumin is the most abundant blood plasma protein and is produced in the liver and forms a large proportion of all plasma protein.⁸ Following intravenous administration of drugs more than 90% of metal based drugs are covalently bound to the plasma proteins.

N, N'–Bis(salicylidene)–1,2–phenylenediamine (salphen), one of the most popular symmetrical tetradentate ligands and its analogue, salen form complexes with various metal ions and these metal–salen (salphen) complexes find extensive applications in catalysis and as sensor and drug.^{9–11} Salphen ligand readily

combines with vanadium salts and forms oxovanadium complexes which show binding properties with proteins.^{12,13}

Bovine serum albumin (BSA), the major soluble protein, serves as a transporter of a variety of endogenous and exogenous ligands such as fatty acids, steroids, drugs, metal ions and metabolites.¹⁴ BSA has 80% similarity to HSA in the structure with a major difference in the number of tryptophans while HSA has only one tryptophan, BSA has two. BSA is usually selected for the protein binding studies because of its abundance, low cost, and ease of purification, stability, medical importance and ligand binding properties.^{15, 16} BSA binds and neutralizes endogenous and exogenous toxins by means of hydrogen bonding, hydrophobic, electrostatic and metal interaction. When BSA binds with metal ions, binding occurs through the interaction with nitrogen atoms derived from amino group, as imidazole group of histidine and different peptide residues.¹⁷ Numerous enzymes and proteins require metal ions for their biological function and identification of the metal binding sites on biomolecules is essential for understanding their metallobiochemistry.¹⁸

Ping et al¹⁹ reported the interaction of Schiff–base ligand and its Fe(II), Cu(II) and Zn(II) complexes with BSA by tryptophan fluorescence quenching method. The Cu(II) complex synthesized by Shahabadi and Maghasudi²⁰ strongly quenches the intrinsic fluorescence of BSA through a static quenching process and the hydrophobic and hydrogen bonding interactions play a major role in BSA–Cu complex association. Lo et al^{21–23} and Rajagopal and co-workers^{24–26} have extensively studied the BSA binding properties of luminescent Re(I)–complexes and used this for cell imaging studies. Rajagopal and co-workers have also used ruthenium(II)–bipyridine–calixarene²⁷ and ruthenium(II)–

aptamer systems^{28, 29} recently in our laboratory to investigate conformational changes of proteins.

Ferrer et al³⁰ investigated the ability of vanadates and vanadyl ions to produce conformational changes in BSA at physiological pH. Chakravarty and co-workers³¹ studied the binding property of oxovanadium complexes of phenanthroline bases to BSA through the tryptophan fluorescence quenching experiments. Vanadium binds with proteins to form vanadium–protein complexes, vanabins, which have recently been isolated from the vanadium-rich ascidian.³² Each molecule of vanabin 1 can bind to ten V(IV) ions and of vanabin 2 can bind to 20 V(IV) ions.

In the present study, eight salphen ligands and their V(IV) complexes were synthesized and their interaction with BSA studied by absorption and fluorescence titration experiments to estimate the binding constants. Fluorescence spectral measurements carried out by varying the concentration of BSA and also of both salphen ligands and the V(IV)–salphen complexes indicate strong fluorescence resonance energy transfer (FRET) from BSA to the ligand/metal–salphen complex. This interaction leads to conformational changes in BSA realized through circular dichroism as well as EPR spectroscopy.

The behavioral study of these oxovanadium(IV)–salphen complexes on bovine serine albumin was carried out by using different in-silico computational methods to understand the atomic level interaction pattern of our synthesized molecules in the target site where initially the complexes were optimized by using density functional theory of Jaguar after which were docked against BSA using Glide whose poses were scored to obtain ΔG by Prime MM-GBSA. This ligand–receptor complex stability was investigated by explicit molecular dynamics at physiological pH 7.4. The cytotoxicity of these complexes against the AGS gastric cell lines assessed by MTT assay shows that V(IV)–salphen complexes have excellent cytotoxic activity with potential applications for cell imaging.

Experimental section

Materials

Salicylaldehyde (SRL), 5–chloro, 5–bromo, 5–nitro, 5–methyl, 5–methoxy, 3, 5–dichloro and 3, 5–di-*tert*-butyl salicylaldehyde (Aldrich) were of high purity and used as such. 1, 2–Phenylenediamine was purchased from Fluka, BSA from Ocimum Bioscience and vanadyl sulphate from Aldrich and used as such for the synthesis and spectral studies.

Preparation of salphen ligands and oxovanadium(IV)–salphen complexes

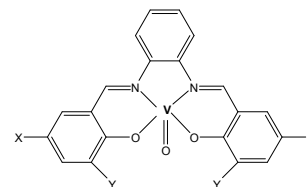
The salphen ligands and the oxovanadium(IV)–salphen complexes were prepared by the reported procedures.^{33, 34} Among the synthesized compounds, Complexes **I**, **II**, **VII**, **VIII** were known³⁵ and the complexes **III**, **IV**, **V**, **VI** were newly synthesized and all the complexes were characterized by NMR, IR, and mass spectra. The structure of oxovanadium(IV)–salphen complexes used in the present study is shown in Chart 1.

Methods

Standard stock solutions of salphen ligands, V(IV) complexes and BSA were prepared in CH₃CN and of BSA in phosphate buffer pH 7.4. All the reactions involving BSA were carried out

in aqueous medium (98% water–2% acetonitrile (v/v)) at pH 7.4 using phosphate buffer to maintain the pH.

The UV–visible absorption spectral measurements were carried out using Agilent 8453 diode array spectrophotometer. ¹H and ¹³C NMR for the salphen ligands in CDCl₃ were obtained using Bruker 300MHz spectrometer. The infrared spectra of the ligands and complexes were recorded in a JASCO FT IR–410 spectrophotometer in solid phase as KBr pellets.



- | | |
|----------------------------|------------------------------|
| I) X=Y=H | II) X=Cl, Y=H |
| III) X=Br, Y=H | IV) X=NO ₂ , Y=H |
| V) X=CH ₃ , Y=H | VI) X=OCH ₃ , Y=H |
| VII) X=Y=Cl | VIII) X=Y= <i>t</i> -butyl |

Chart 1. Structure of oxovanadium(IV)–salphen complexes.

EPR spectra were recorded using Bruker EMX Micro premium X spectrometer at liquid N₂ and at room temperature at X– band (9.4 GHz). The cyclic voltammograms were recorded using a CHI760D Electrochemical Workstation, CH Instruments, Inc., USA. Glassy carbon, platinum wire and Ag/AgCl were used as working, supporting and reference electrodes respectively. The mass spectra were recorded using Quattro LC triple–quadrupole mass spectrometer. The fluorescence spectral measurements were recorded using JASCO FP–6300 spectrofluorimeter. The circular dichroism (CD) data were obtained using JASCO J 810 spectropolarimeter at room temperature.

Computational studies

The oxovanadium(IV) complexes were sketched using Maestro 9.3 (Maestro version 9.3, Schrödinger, LLC, New York, NY, 2012) and prepared by ligprep (LigPrep, version 2.5, Schrödinger, LLC, New York, NY, 2012) at biological pH, generating the low energy ring conformations 1 per ligand. These molecules were further processed using quantum mechanical optimizations by Jaguar (Jaguar, version 7.9, Schrödinger, LLC, New York, NY, 2012) using density functional theory. The energy minimized complexes were used as input for docking studies. Docking was performed using our optimized complexes and the X– ray crystal structure of BSA with resolution of 2.7 Å retrieved from PDB id: 3V03³⁶. All the heteroatoms were removed from the 3V03 pdb, to make complexes receptor free before docking. The possible binding sites of BSA were searched using Q–site finder.³⁷ Among the various druggable sites, the site with higher score used as target site to generate the receptor grid for docking. Docking was performed using the energy minimized oxovanadium(IV)–salphen complexes against BSA protein (PDB id: 3V03), using Glide (Glide, version 5.8, Schrödinger, LLC, New York, NY, 2012.) by means of XP precision mode. The docked protein– V(IV) complex structure corresponding to the minimum score was chosen and composite coordinates of the complexes generated. The binding energy was computed and the ligand binding pattern was observed.

The docked molecules were further subjected to molecular dynamics using Desmond where the complex system was built using predefined solvation (TIP3P water) with box shape orthorhombic with box volume (806898 \AA^3) using partial charges from structures with force field of OPLS 2005. The solvated complexes were further minimized with maximum iterations of 2000 with convergence criteria of 1.0 kcal/mol/\AA and then minimized solvated receptor complex was processed for dynamics with ensemble class NPT of temperature 300.0 (K) and pressure (bar) 1.01325 simulation time of 10 ns .^{38,39}

In vitro antitumor activity

Cell Culture

The AGS gastric cancer cell line was obtained from NCCS (National Centre for Cell Science, Pune). The cells were cultured in Dulbecco's Modified Eagle's Medium (DMEM, Sigma Aldrich) which was supplemented with 10% fetal bovine serum. The cells were grown at 37°C in a humidified 5% CO_2 atmosphere.

Cell viability assay

The cytotoxicity of salphen ligands and oxovanadium(IV) complexes were tested against AGS gastric cell lines using 3-(4,5-dimethylthiazole-2-yl)-2,5-diphenyl tetrazolium bromide (MTT) assay.⁴⁰ The cells were seeded into a 96-well plate at a density of 1.5×10^4 cells/well and incubated in medium containing salphen ligands and the oxovanadium(IV) complexes at concentrations ranging from 0.01 to $100 \mu\text{M}$ for 48h. Triplicate wells were maintained for each treatment. To each well $100 \mu\text{L}$ of MTT was added and the plates were incubated at 37°C for 4h to allow MTT to form formazan crystals by reacting with metabolically active cells. The medium with MTT was removed from the wells. Intracellular formazan crystals were dissolved by adding $100 \mu\text{L}$ of DMSO to each well and the plates were shaken for 10min. The absorbance was read at 570nm and 630nm using an enzyme linked immunosorbent assay (ELISA) reader and the cell images were examined using fluorescence microscope (Nikon, Japan). The percentage of survival was calculated using the formula, % survival = [live cell number (test)/ live cell number (control)] $\times 100$.

Results and discussion

NMR spectra

The ^1H and ^{13}C NMR spectral data of the salphen ligands recorded in CDCl_3 are presented in the Tables S1 and S2 in the supporting information. The values of chemical shifts obtained were very close to those of Schiff-base ligands reported in the literature.⁴¹

FT-IR spectral data

The data on the important infrared spectral bands of the ligands and the metal complexes are presented in Tables S4 and S5 in the supporting information. The absorption bands due to the amino group disappeared in the FT-IR spectra of the ligands, which showed that the amino groups in the diamine condensed with the aldehyde. All the salphen ligands gave a sharp and strong band due to $\nu(\text{C}=\text{N})$ of the azomethine group at $1601\text{--}1620 \text{ cm}^{-1}$ while the corresponding bands in the complexes were observed in the $1595\text{--}1620 \text{ cm}^{-1}$ range.⁴² The observed shift of $\pm 10 \text{ cm}^{-1}$ to a lower frequency of the $\nu(\text{C}=\text{N})$ in the complexes indicates a decrease in the bond order of $\text{C}=\text{N}$ due to the coordination of azomethine nitrogen to the metal ion. The bands due to $\nu(\text{V}-\text{N})$ and $\nu(\text{V}-\text{O})$ observed only in the complexes, occurred at $515\text{--}542 \text{ cm}^{-1}$ and $419\text{--}495 \text{ cm}^{-1}$ respectively.⁴³

Mass spectra

The mass spectra of the ligands and the complexes were recorded and the mass values were similar to that of the formula weight and presented in the Table 1 and the mass spectra of the ligand **I** and complex **I** are shown in Fig. S1 and S2 of the supporting information.

EPR spectra

The oxovanadium(IV)–salphen complexes in toluene solution at room temperature exhibit eight equally spaced lines due to the hyperfine interactions of the unpaired electrons with the vanadium nucleus (^{51}V , $I=7/2$).^{44,45} The g -values (given in Table S3 in the supporting information) indicate that the vanadyl ion (VO^{2+}) is in a distorted octahedral coordination environment and the unpaired electron is located mainly in the $d_{x^2-y^2}$ orbital.⁴⁶ The EPR spectral data for the oxovanadium(IV)–salphen complexes are in good agreement with published data for similar complexes.^{47,48} The data are given in the supporting information (Table S3) and the EPR spectra of the complex **I** at room temperature and at 77K (LNT) are shown in the Fig. 1.

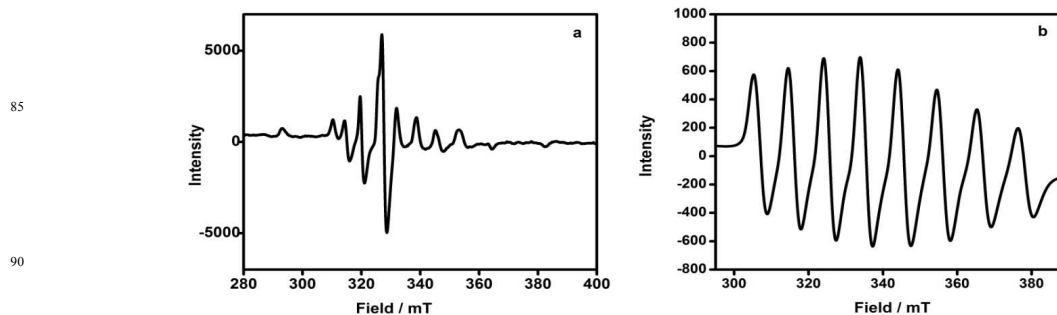


Fig. 1 EPR spectrum of **I** (A) at LNT (B) at room temperature.

Cyclic voltammetry (CV)

Cyclic voltammetric data for three complexes **I**, **III** and **VI** in DMF have already been reported.⁴⁹ As the present study has been

carried out in CH_3CN , voltammetric measurements of all V(IV) –salphen complexes, **I–VIII** were performed at room temperature in CH_3CN with 0.1 M tetrabutylammonium perchlorate as the

supporting electrolyte. The electrochemical data for the complexes **I** to **VIII** are given in Table 1 and the cyclic voltammograms for the oxovanadium salphen complexes are shown in the Fig. S3 of the supporting information. For the parent complex **I** an oxidation peak is observed at 0.71V and VO(salphen) is oxidized to [VO(salphen)]⁺ in a fully reversible one electron step. Upon reversal of the scan direction, the V(V) complex is reduced at lower potential at 0.64V. Comparison of our data with the data reported in DMF indicate that the $E_{1/2}$ values are found to be 0.15 V lesser in DMF than the values obtained in CH₃CN which may be attributed to solvent effect. These results reveal that the redox process for all of the vanadyl-salphen complexes under study is the one-electron transfer reaction. The $E_{1/2}$ values of all VO(salphen) complexes were

plotted as a function of Hammett's σ_p parameter for the substituents X in [VO(5-Xsal)] and the plot is linear (Fig. S4 of the supporting information). A linear relationship with the slope value (+0.22) obtained in the $E_{1/2}$ versus σ_p plot (Fig. S3) supports the postulation that the electronic effect of substituents is transmitted through the ligand to the metal centre of the complexes. Similar results have been reported previously by us for analogous metal-salen systems [metal-Mn(III), Fe(III), and Cr(III)].⁵⁰⁻⁵⁴ The Hammett-type relationship found between $E_{1/2}$ values of metal-salphen complexes and the appropriate *para*-substituent parameters,⁵⁵ reflects the variation of the redox potential of the metal complex as a function of the electron donating or withdrawing ability of the substituents at positions 5, 5' of salphen ligand.

Table 1. UV-visible^a, ESI-MS^b, FT-IR, CV^c data for oxovanadium(IV)-salphen complexes at 300K. a & c = CH₃CN; b = CH₃OH.

Complex	λ_{\max} (nm)	ϵ at MLCT ($M^{-1} cm^{-1}$)	ESI-MS	FT IR (cm^{-1})			$E_{1/2}$ (V)
				$\nu_{C=N}$	ν_{C-O}	$\nu_{V=O}$	
I	242,314,396	17700	382	1607	1196	978	0.68
II	245,314,405	10800	450	1607	1280	970	0.75
III	248,304,408	10300	541	1605	1246	968	0.75
IV	248,335,397	19280	472	1618	1298	978	–
V	240,324,409	17100	410	1620	1263	978	0.60
VI	242,335,431	10200	442	1595	1220	974	0.56
VII	249,331,416	9900	519	1603	1227	987	0.80
VIII	250,327,417	16000	606	1601	1250	976	0.52

UV-visible absorption spectra

The UV-visible absorption spectra of the V(IV) complexes recorded in CH₃CN at room temperature show the λ_{\max} values in the range 200–480 nm similar to the values reported in the literature for other metal-salphen complexes.^{56, 57} The strong high energy absorption bands at 300–350 nm are assigned to the ligand centered (LC) $\pi \rightarrow \pi^*$ transition and low energy absorption bands at 400–480 nm due to spin allowed ligand to metal charge transfer (LMCT) transition from $\pi^*(\text{dimine}) \rightarrow d\pi(V)$. The overlay absorption spectra of ligands and complexes are shown in the Figure S5 of the supporting information. The introduction of electron donating groups in the salphen ligand results in the maximum red shift (i.e. ~10 to 25 nm) in the λ_{\max} value of V(IV)-salphen complex implying that as the degree of conjugation increases the $^1\pi-\pi^*$ energy level is lowered leading to the red shift.⁵⁸ On the other hand the introduction of electron withdrawing group in the salphen ligand results in a minimum red shift in the λ_{\max} value and the values are listed in Table 1. Similar results were observed by us on other metal-salen complexes.^{9, 50-54}

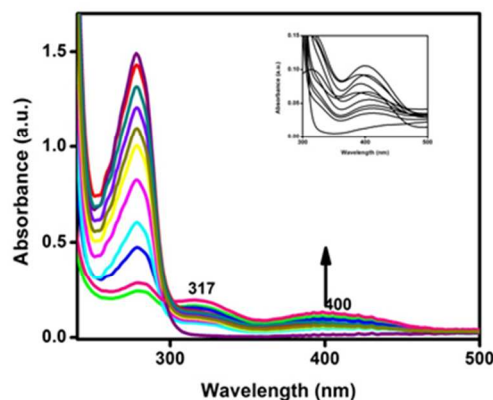


Fig. 2 Absorption spectral changes of complex **I** (2 μ M) with the addition of BSA (0–20 μ M) in 2%CH₃CN–98% H_2O (v/v), pH=7.4 at 300 K.

Binding of salphen ligands and oxovanadium(IV)-salphen complexes with BSA

For the characterization of synthesized V(IV) complexes spectral studies UV-vis and EPR and other (CV) studies have been carried out in different organic solvents but their binding studies

with BSA in aqueous buffer medium maintaining the pH at 7.4. In the aqueous medium the axial position of the metal-salen complexes is occupied by water molecule. Thus we presume that the actual species in the aqueous medium is [VO(salphen)(H₂O)] similar to other recent studies.⁵⁹ Generally V(IV) complexes are sensitive to oxygen and oxidized to V(V). To check the stability of V(IV) complexes in the presence atmospheric oxygen we recorded the absorption spectra of complex **I** in the absence and presence of nitrogen atmosphere. Similar results were observed in the aerobic and anaerobic conditions. These results confirm the stability of synthesized vanadium complexes under the experimental conditions used in the present study.

Absorption spectral study

In order to learn the strength of the binding of salphen ligands as well as oxovanadium(IV)–salphen complexes, **I–VIII** with BSA, the absorption spectral titrations were carried out in the aqueous medium [2%CH₃CN–98%H₂O (v/v)] at pH 7.4. The concentration of the salphen ligands and oxovanadium(IV)–salphen complexes used for absorption spectral study was fixed at 2 μM and the BSA protein concentration was varied from 0–20 μM in 0.1 M phosphate buffer pH 7.4. On increasing the concentration of BSA, apart from an increase in the absorbance of BSA at 280 nm, a substantial change in the absorption intensity of the V(IV) complex with a blue shift of ~ 50 nm from 450 → 400 nm is noted which shows the strong binding of V(IV) complex with BSA. At this juncture it is appropriate to comment on the nature of binding of V(IV) complex with BSA. Our earlier studies^{34, 52} show that the binding of N-oxides and imidazole at the axial position of metal - salen complex leads to substantial red shift in the λ_{max} value. The substantial blue shift observed here in the presence of BSA prompts us to propose that the binding of the protein with the V(IV) complex is not due to

the binding in the axial position of the complex. Recent studies^{60, 61} indicate that V(IV)–salphen complexes undergo binding with other molecules through hydrogen bonding and hydrophobic interactions which also get support from theoretical studies (*vide infra*). Thus we propose that in the present study also BSA binds with the V(IV) complexes through these non-covalent type of interactions. The absorption spectral changes of V(IV) complex **I** on the addition of various concentration of BSA are shown in the Fig.2. Though BSA has no absorption at 315 and 400 nm, addition of BSA leads to a substantial increase in the absorbance at these wavelengths and these spectral changes have been used for the calculation of the binding constant (K) of V(IV) complex with BSA by using eq.(1).⁶²

$$A_0/A - A_0 = (\epsilon_{BSA}/\epsilon_C) + (\epsilon_{BSA}/\epsilon_C \cdot K) \times 1/[BSA] \quad (1)$$

Here, A₀ and A are the absorbance of oxovanadium(IV)–salphen complex at 400 nm in the absence and presence of BSA, ε_V and ε_C are the molar extinction coefficient of free and the BSA bound V(IV) complex. Thus, from the linear double reciprocal plot of 1/(A–A₀) vs 1/[BSA] the binding constant (K) has been estimated from the ratio of the intercept to the slope. The binding constant values for the binding of ligands and V(IV) complexes with BSA calculated from absorption spectral data are given in Table 2. We have also recorded the absorption spectrum of BSA at different V(IV) concentrations and the results are shown in the supporting information, Fig.S6. The results shown in the Fig. S6 indicate that with the addition of vanadium complex there is an increase in the absorbance at 280 nm (corresponding to the λ_{max} of BSA) apart from an increase in the absorbance at 316 and 396 nm (the λ_{max} values of the vanadium (IV) complex). These results also support the binding of V(IV) complex with BSA.

Table 2. Binding constant for ligands and oxovanadium(IV)–salphen complexes with BSA from absorption and emission spectral studies in 2%CH₃CN–98%H₂O (v/v), pH=7.4 at 300 K.

Ligand	K (M ⁻¹)		Complex	K (M ⁻¹)	
	Absorption	Emission		Absorption	Emission
1	3.1 × 10 ³	7.9 × 10 ³	I	6.7 × 10 ⁴	8.5 × 10 ⁴
2	2.8 × 10 ³	7.3 × 10 ³	II	2.3 × 10 ⁴	5.1 × 10 ⁴
3	4.9 × 10 ³	4.9 × 10 ³	III	1.1 × 10 ⁴	7.0 × 10 ⁴
4	2.4 × 10 ⁴	2.2 × 10 ⁴	IV	3.4 × 10 ⁴	4.2 × 10 ⁴
5	6.8 × 10 ³	9.6 × 10 ³	V	5.9 × 10 ⁴	6.2 × 10 ⁴
6	2.1 × 10 ³	2.4 × 10 ³	VI	6.5 × 10 ⁴	8.4 × 10 ⁴
7	6.7 × 10 ³	7.5 × 10 ³	VII	2.3 × 10 ⁴	4.6 × 10 ⁴ (K _{SV})
8	1.7 × 10 ³	7.1 × 10 ³	VIII	1.6 × 10 ⁴	8.4 × 10 ⁴

70

Fluorescence quenching study

The fluorescence emission spectra of BSA in the absence and presence of salphen ligands and oxovanadium(IV)–salphen complexes were recorded with excitation at 280 nm. The concentrations of the salphen ligands and oxovanadium(IV)–salphen complexes used for emission spectra were 0–30 μM , in 0.1 M phosphate buffer pH 7.4, and the concentration of BSA was fixed at 5 μM . The fluorescence spectral results collected in Fig.3 show that the fluorescence intensity of BSA is decreased significantly with a blue shift from 338 to 332 nm in λ_{max} of tryptophan fluorescence in the presence of ligand **1** and a blue shift of 338 to 335 nm for complex **I**. These fluorescence spectral changes also imply that the ligand as well as the V(IV) complex binds strongly with BSA.⁶³ An interesting observation is that on increasing the concentration of ligand/V(IV) complex apart from the fluorescence quenching of BSA at 340 nm the luminescence band corresponding to the ligand / V(IV) complex is regenerated at 450 nm and the intensity of this band increases with an increase in the concentration of the quencher. In order to examine the quenching mechanism, the fluorescence quenching is analyzed by the Stern–Volmer equation (2)^{64, 65}

$$F_0/F = 1 + k_q \tau_0 [Q] = 1 + K_{sv} [Q] \quad (2)$$

where F_0 and F are the fluorescence intensities of BSA in the absence and presence of the quencher (ligand/V(IV) complexes), k_q is the bimolecular quenching constant, τ_0 is the lifetime of fluorophore in the absence of quencher, K_{sv} is the Stern-Volmer quenching constant. The Stern-Volmer plot shown in the inset of Fig.3b exhibits an upward curvature, concave toward the Y-axis at high [quencher]. This non-linear Stern-Volmer plot indicates that more than one process contribute to the overall quenching of BSA. It has been reported in many cases that fluorophores can be quenched both by collision (dynamic quenching) and by complex formation with the same quencher (static quenching). In the case of competitive quenching, F_0/F is related to $[Q]$ by the modified Stern-Volmer equation (eq.3).⁶⁶

$$(F_0/F) = (1 + K_D [Q]) (1 + K_S [Q]) \quad (3)$$

where K_S and K_D are the static and dynamic quenching constants, respectively. The non-linearity and the upward curvature of the plot suggest the occurrence of combined quenching (both dynamic and static) process. The K_D , K_S and quenching constant (k_q) values for the interaction of BSA with salphen ligands and oxovanadium(IV)–salphen complexes are given in Table S6 in the supporting information. The high value of quenching rate constant, k_q (10^{12} – $10^{13} \text{M}^{-1} \text{s}^{-1}$) indicates efficient bimolecular quenching along with binding.⁶⁷ The Stern-Volmer plots of ligands and complexes are shown as insets in Fig. 3. The non-linearity of the Stern-Volmer plots is due to the ground state complex formation between V(IV) complex and BSA. This complex formation is facilitated through hydrogen bonding and hydrophobic interactions. The UV-visible absorption spectral study compels us to exclude axial binding and ligand substitution reactions of BSA. The docking studies also support this

postulation (*vide infra*). The non-linear Stern–Volmer plots and high quenching constant value of 10^{12} – $10^{13} \text{dm}^3 \text{mol}^{-1} \text{s}^{-1}$ indicate that⁶⁸ strong ground state complex formation contributes significantly to the overall quenching of fluorescence intensity of BSA. The complex **VII** shows a different quenching behavior, a downward curvature in Stern-Volmer plot which indicates that buried tryptophan residues are likely exposed to the quencher. Docking studies also confirmed this unique behavior of complex **VII** which shows the contributions of both hydrogen bonding and hydrophobic interactions to the binding process.

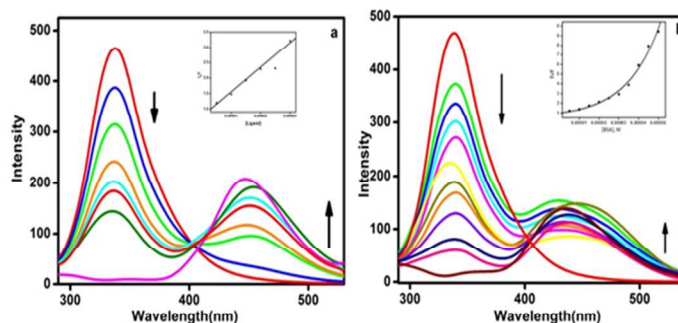


Fig. 3 Fluorescence spectra of BSA (5 μM) with the addition of a) ligand **3** (0–30 μM), b) **V** (0–30 μM) in 2% CH_3CN –98% H_2O (v/v), at 300 K, $\lambda_{\text{ex}} = 280 \text{ nm}$, pH = 7.4 (Inset shows the corresponding Stern-Volmer plots).

Fluorescence resonance energy transfer (FRET) from BSA to the salphen ligands / oxovanadium(IV)–salphen complexes

The fluorescence spectral changes indicate the initial quenching followed by the regeneration of luminescence of salphen ligand. On the other hand in the presence of V(IV) complex the fluorescence of BSA is quenched and the luminescence of V(IV)–salphen complex is also observed with a red shift at high concentration of V(IV) complex. This quenching of fluorescence of BSA and formation of luminescence of the ligand and V(IV) complex is proposed to be due to the energy transfer from the excited state BSA to the ligand / V(IV) complex (FRET) because of the strong overlap of fluorescence spectrum of tryptophan (Trp) of BSA and the absorption spectrum of V(IV) complex.(Fig.4)

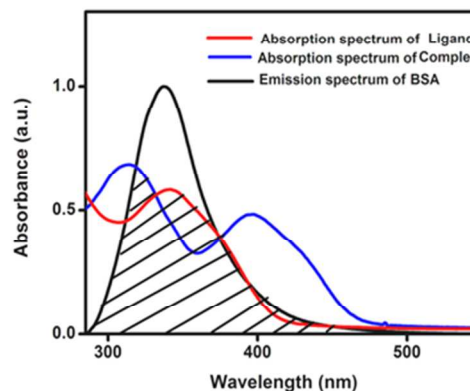


Fig. 4 Spectral overlap of emission spectrum of BSA and absorption spectrum of ligand **1** and complex **I**.

Fluorescence resonance energy transfer (FRET) is a non-radiative spectroscopic method that can be used to monitor the proximity and the relative orientation of the fluorophores.⁶⁹ FRET process occurs when there is an overlap between the emission spectrum of the donor (BSA) and the absorption spectrum of the acceptor (salphen ligand / oxovanadium complex). Spectral overlap between the fluorescence spectrum of BSA and the UV-visible absorption spectrum of complex **I** / ligand **I** is shown in Fig. 4. According to the Forster's theory, the energy transfer efficiency (E) is defined by equation (4)

$$E = R_0^6 / R_0^6 + r^6 = 1 - (F/F_0) \quad (4)$$

where F and F₀ are the fluorescence intensity of BSA after and before the addition of oxovanadium complex respectively, r represents the distance between donor and acceptor during the energy transfer process, and R₀ is the critical distance when the transfer efficiency equals to 50%. The value of R₀ is calculated using the equation (5)

$$R_0 = 8.79 \times 10^{-25} k^2 n^{-4} \phi J \quad (5)$$

where, k² is the orientation factor related to the geometry of donor-acceptor dipole, n is the refractive index of medium, φ is the fluorescence quantum yield in the absence of energy transfer and J is the spectral overlap integral between the fluorescence spectrum of donor and the absorption spectrum of acceptor. The value of J can be calculated by the equation (6)

$$J = \int F(\lambda) \varepsilon(\lambda) \lambda^4 d\lambda / \int F(\lambda) d\lambda \quad (6)$$

where F(λ) is the fluorescence intensity of donor at wavelength λ, ε(λ) is the molar absorption coefficient of acceptor at wavelength λ. The calculated J, R₀ and r values using k² = 2/3, n = 1.336,

and φ = 0.15 are shown in Table S7 in the supporting information and are similar to the values obtained for the binding of Pt(II) complexes with BSA.⁷⁰ From the calculated data, we observe that the donor to acceptor distance is in the range 1.4–3.5 nm, which is in accordance with conditions of Forster's non-radiative energy transfer theory. These results indicate that the energy transfer between BSA and the salphen ligands/oxovanadium complexes occurs with high probability.⁷¹ Similar type of energy transfer mechanism has already been reported when Stern-Volmer plot is non-linear.⁷² For complex **VII**, the r value is higher (3.5 nm) than that of other complexes which may be due to the binding of complex **VII** with buried tryptophan residues of BSA. Due to the interface binding for the complex **VI**, the r value is minimum (1.4 nm) when compared with other complexes. These proposals also get support from docking studies.

The salphen ligands and the oxovanadium(IV)-salphen complexes are found to be luminescent and thus the fluorescence titrations are carried out by keeping the concentration of salphen ligand and oxovanadium(IV)-salphen complex fixed and varying the concentration of BSA. In this case, luminescence enhancement at the emission maximum of ligand/V(IV) complex is observed. All the oxovanadium(IV)-salphen complexes except complex **VII** (shows quenching) show an enhancement in their emission intensity at ~490 nm on the addition of BSA (Fig. 5b). The luminescence enhancement of V(IV) complex is proposed to be due to the energy transfer from the excited state of BSA to V(IV) complex in the BSA-V(IV) adduct. The fluorescence spectra of ligand **I** and the vanadium(IV) complex **VIII** in the presence of different concentrations of BSA are shown in Fig. 5.

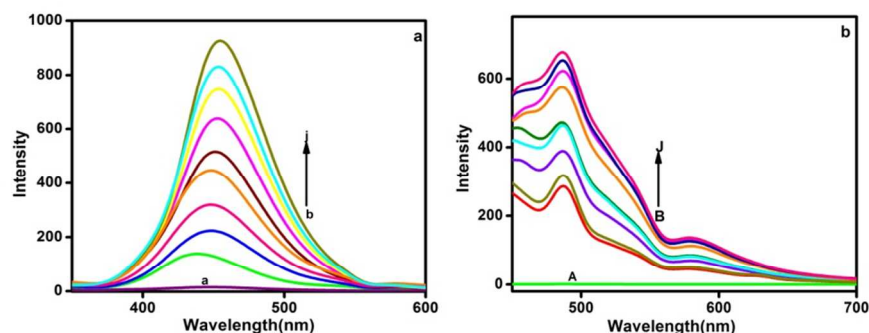


Fig. 5 Fluorescence spectra of a) ligand **I** (5 μM) (λ_{ex} = 330 nm) a=only BSA, b) complex **VIII** (5 μM) (λ_{ex} = 417 nm) A=only BSA, with the addition of BSA (0–40 μM) in 2% CH₃CN–98% H₂O (v/v), pH=7.4 at 300 K.

In the case of parent ligand, on the addition of various concentration of BSA to the fixed concentration of the ligand there is luminescence enhancement as well as a large red shift *i.e.* from 437 nm to 454 nm. This shows the stabilization of emissive state due to strong binding of ligand with BSA.

The binding constants were calculated using modified Benesi-Hildebrand equation (7)⁷³ and are given in the Table 2 and the plots are shown in Fig. S7 in the supporting information.

$$F_0 / F - F_0 = b / (a - b) (1/K_a [BSA] + 1) \quad (7)$$

where F and F₀ are the luminescence intensity of V(IV) complex in the presence and absence of the BSA respectively, K_a is the binding constant, a and b are constants. It is interesting to note that the binding constant values estimated by the absorption as well as the emission spectral study agree well. The binding constant values of the V(IV) complexes are one order higher than that of the ligands. These higher binding constants observed with

V(IV) complexes indicate that the metal complexes have better binding capacity than the ligands with BSA. This may be due to the hydrogen bonding between the amino groups of the proteins and the phenoxide oxygen V=O of the complexes similar to the binding of small molecules with V(IV)–salphen complexes reported recently.⁶⁰

Synchronous fluorescence spectroscopy studies

Synchronous fluorescence spectra are used to characterize the interaction between fluorescent probe and proteins.⁷⁴ When $\Delta\lambda$ of 15 nm is used, the obtained synchronous fluorescence spectrum indicates the spectral property of tyrosine residues, whereas $\Delta\lambda$ of 60 nm indicates that of tryptophan residues.⁷⁵ The maximum emission wavelengths of tryptophan and tyrosine residue in the protein molecule are related to the polarity of their surroundings; changes of the emission maximum wavelengths can reflect changes of protein conformation. The effect of V(IV) complexes on the synchronous fluorescence spectrum with $\Delta\lambda = 60$ nm and $\Delta\lambda = 15$ nm is shown in Fig. S8 in the supporting information. A slight red shift from 341 to 343 nm when $\Delta\lambda$ is equal to 60 nm and shows similar shift from 302 to 304 when $\Delta\lambda = 15$ nm are observed. The red shift in the synchronous fluorescence spectrum points to a slight change in the conformation of BSA and the polarity around the tryptophan and the tyrosine residues indicating a decrease in the hydrophobicity.⁷⁶ Similar results have been observed when the medicinally important Pt(II) complexes bind with BSA.⁷⁰

Circular Dichroism Spectra

Circular dichroism is a sensitive technique to monitor conformational changes of protein upon interaction with small molecules. The structural changes of BSA and the efficiency of binding of BSA with oxovanadium(IV)–salphen complexes were studied using circular dichroism spectra and α -helical contents were calculated using the equations (8–10) and the values listed in Table S8.

BSA shows two negative bands, located at 208 and 222 nm characteristics of the α -helical structure.⁷⁷ The main information provided by the CD spectral study is the changes in the protein secondary structure upon ligand/V(IV) complex–protein interaction. The CD spectral data are expressed in terms of mean residue ellipticity (MRE) in $\text{deg cm}^2 \text{dmol}^{-1}$, according to the equation (8).

$$\text{MRE} = \text{observed CD (mdeg)} / C_p n l \times 10 \quad (8)$$

where C_p is the molar concentration of the protein, n is the number of amino acid residues of the protein and l is the path length.

The α -helical contents of free and bound BSA were calculated from mean residue ellipticity values at 208 nm using the equation (9)⁷⁸

$$\alpha\text{-helix (\%)} = [-\text{MRE}_{208} - 4000 / (33000 - 4000)] \times 100 \quad (9)$$

In eq.(9) 4000 is the MRE of the β -form and random coil conformation cross at the observed wavelength and 33000 is the

MRE value of a pure α -helical content at the observed wavelength. Similarly the α -helix content of free and combined BSA were calculated from mean residue ellipticity values at 222nm using the equation (10)⁷⁹

$$\alpha\text{-helix (\%)} = [-\text{MRE}_{222} - 2340 / 30300] \times 100 \quad (10)$$

The CD spectra of BSA in the absence and presence of V(IV) complex in the visible region was also recorded and the results displayed in the Fig.S9. BSA shows positive signal in the region 620-790nm. Addition of V(IV) complex leads to a shift in the wavelength and an increase in the intensity. This also indicates the binding of V(IV) complex with BSA. The peak at 546nm corresponds to the d-d band of V(IV) complex.

Conformational changes of BSA

The absorption and emission spectral studies of oxovanadium(IV)–salphen complexes in the presence of BSA as well as CD studies confirm the interaction between them. It is important to examine how the structure of BSA is affected in the presence of oxovanadium(IV)–salphen complexes. When the ligands bind to a globular protein, the intermolecular forces responsible for maintaining the secondary and tertiary structures can be altered, resulting in a conformational change of the protein.⁸⁰ The luminescence quenching along with the blue shift from 338 to 335 nm observed for BSA in the presence of V(IV) complexes suggest that the BSA–V(IV) complex combination has changed the microenvironment of BSA. BSA has a high percentage of α -helical structure which shows the characteristic strong double minima CD signals at 208 and 222 nm. (Fig. S8). The CD spectra of BSA in the presence and absence of oxovanadium(IV)–salphen complexes show similarity in shape. This indicates that the structure of BSA is predominantly α -helical even after binding to the complex. However, it is noticed that the intensity of peaks at 208 and 222 nm decreased substantially upon the addition of various amounts of oxovanadium(IV)–salphen complexes to free protein (Fig. S8). This clearly indicates the changes in secondary structure of protein as evident from the decrease in α -helical content of protein.⁸¹ In the present study, the α -helicity of BSA decreased from 59% to 28% in the presence of complex I. Thus the results of CD spectra indicate that the conformation of the BSA molecule is changed significantly in the presence of oxovanadium(IV)–salphen complex.

EPR data

The EPR spectra of oxovanadium(IV)–salphen complexes I and VIII recorded in the presence of various concentrations of BSA are shown in Fig.6. With the addition of various concentrations of BSA, the intensity of the peaks of V(IV) complexes get decreased in all the complexes. However, it is interesting to see a substantial change in the nature of EPR spectrum of complex I which shows a slight shift in the field in addition to the decrease in the intensity. These changes in the EPR spectrum of V(IV) complex on the addition of BSA indicate strong binding accompanying the change of geometry of oxovanadium(IV)–salphen complexes due to binding with BSA. On the other hand the change in the EPR

spectrum of complex **VIII** is marginal on the addition of BSA. The different behavior of complexes **I** and **VIII** towards BSA indicates the importance of steric effect on the efficiency of binding of these metal complexes with BSA.⁸² Complex **VIII** carries bulky *tert*-butyl groups in the salphen ligand. The hydrogen bonding to the phenoxide oxygen is perturbed by the *tert*-butyl groups. In the previous sections we have pointed out that hydrogen bonding and hydrophobic interactions are mainly responsible for the strong binding of V(IV) complexes with BSA. The effect of BSA on the EPR spectra of complexes **I** and **VIII** also support the proposal of hydrogen bonding is one of the main interactions responsible for the binding of V(IV)-salphen complexes with BSA. Recent reports^{60, 82} highlight the effect of binding of epoxides on the EPR spectra of V(IV)-salphen complexes. Our results are similar to the observations reported there. In order to get more details on the nature of V(IV)-salphen complex-BSA adduct from EPR a more detailed study is required which will be taken up in the future.

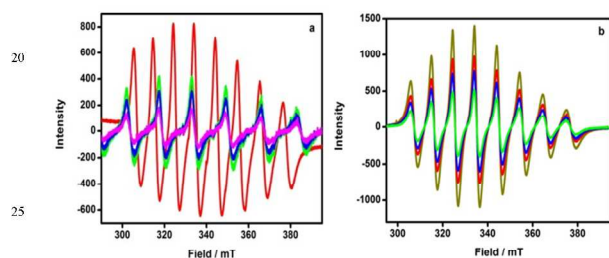


Fig. 6 EPR spectra of a) complex **I** (5 μM) b) complex **VIII** (5 μM) 2%CH₃CN-98%H₂O (v/v), with addition of BSA (0-15 μM) pH=7.4 at 300 K.

In-silico studies

The 3D structure reveals that the BSA is made up of three homologous domains (I, II, and III): I (residues 1-183), II (184-376) and III (377-583). Each domain contains two sub domains (A and B), and they are divided into nine loops by 17 disulfide bonds, each one formed by six helices, and its secondary structure is dominated by α -helix as reported earlier.^{83, 84, 85} BSA can bind with many drugs in several binding sites and the principal regions of drug binding to BSA are located in the hydrophobic cavities in sub domains IIA and IIIA.⁸⁶

The possible drug binding site in BSA was investigated by sitemap (SiteMap, version 2.6, Schrödinger, LLC, New York, NY, 2012), Q-site finder for pocket detection. The predicted active sites consisted of amino acids such as Phe205, Arg208, Ala209, Lys211, Trp213, Val215, Phe227, Thr231, Val234, Thr235, Asp323, Leu326, Gly327, Leu330, Ser343, Leu346, Ala349, Lys350, Glu353, Ser479, Leu480 and Val481. This system was further subjected to docking studies with the volume score of 1.15608. Molecular docking was employed using Glide to understand the interaction between the oxovanadium complexes **I-VIII** and BSA. Glide approximates a complete systematic search of the conformational, orientational, and positional space of the docked ligand. Selection of the best docked pose is based on empirical and force-field-based terms. The docking of bovine serum albumin with synthesized VO(IV) complexes exhibit well

established bonds with one or more amino acids in the receptor active pocket (Phe205, Arg208, Ala209, Lys211, Trp213, Val215, Phe227, Thr231, Val234, Thr235, Asp323, Leu326, Gly327, Leu330, Ser343, Leu346, Ala349, Lys350, Glu353, Ser479, Leu480, Val481).

All the eight synthesized molecules were docked. Fig. 7 shows the docked image of complex **VI**. Table 3 shows the binding energy of the synthesized VO(IV) complexes with BSA.

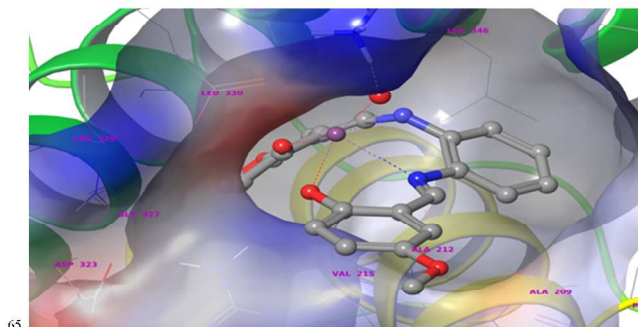


Fig.7 Docking pose of the complex **VI** with Bovine serum albumin. Residues surrounding the binding sites are highlighted

In silico studies revealed that all the synthesized molecules showed good binding energy toward the target BSA protein ranging from -46 to -69 kcal mol⁻¹. The free energy of binding, ΔG^0 is based on empirically derived terms which represent common contributions such as the hydrophobic effect, hydrogen bonding and conformational entropy. The affinity can be quantified⁸⁷ using the binding free energy, ΔG^0 , which is related to the affinity or binding constant K as:

$$\Delta G^0 = -RT \ln K$$

where, R is gas constant and T is temperature in Kelvin.

A negative free energy (Table 3) indicates favorable interaction between the V(IV) complex and protein and the spontaneity of the complexation. The V(IV) complexes used in this study showed significant interactions in the binding cavity of BSA and the interaction graph is shown in the Fig. S10 in the supporting information. This figure shows that ligand **5** has the strongest binding which is also evident from the binding constant values collected in Table 2. Out of 22 amino acid residues considered for the docking studies, residues carrying Ala, Leu and Asp facilitate strong binding with V(IV) complex. Explicit molecular dynamics simulations of the complex were done in real time in order to understand the nature of interaction. The complex is very stable with RMSD (root-mean-square deviation) of the protein backbone less than 3 Å which reveals that V(IV) complexes have a very stable interaction with BSA as shown in the Fig. S11 in the supporting information. Explicit molecular dynamics simulation of the complex was done in real time in order to understand the nature of the interaction and the video file for the interaction of the complex with BSA is shown in Fig. S12.

This study on the interaction of oxovanadium complexes with BSA helps to understand how the drug molecules may affect the structure of proteins when drugs are introduced to target specific diseases.⁸⁸ It is important to recall that vanadium complexes have

been extensively used as drugs against a number of diseases.^{5, 89}

Table 3. Binding energy of BSA with oxovanadium(IV)–salphen complexes.

Complex	MMGBSA ΔG Bind Packing kcal mol ⁻¹	MMGBSA ΔG Bind Lipophilic kcal mol ⁻¹	MMGBSA ΔG Binding kcal mol ⁻¹	MMGBSA ΔG Bind vdW kcal mol ⁻¹
I	0.099	-32.643	-54.451	-34.973
II	-0.071	-40.426	-68.745	-33.030
III	-0.763	-39.064	-46.269	-41.919
IV	-0.709	-16.374	-53.213	-31.221
V	-0.090	-38.789	-62.846	-34.682
VI	-0.134	-34.136	-62.339	-31.777
VII	0.047	-46.377	-51.540	-42.307
VIII	-0.362	-38.851	-68.085	-43.443

Cytotoxicity assay

Salphen ligands **1–8** and Oxovanadium(IV) complexes **I–VIII** were evaluated for their ability to inhibit the growth of AGS gastric cell lines using MTT assay. The inhibition was expressed as cell viability relative to control without complex treatments. The histograms of cell viability assay for different complexes against AGS gastric cells are shown in the Fig. 8 and the cell images in the Fig. 9.

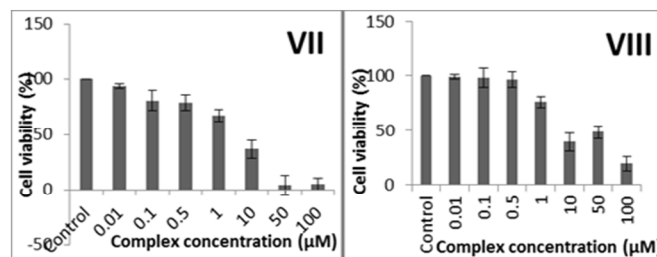
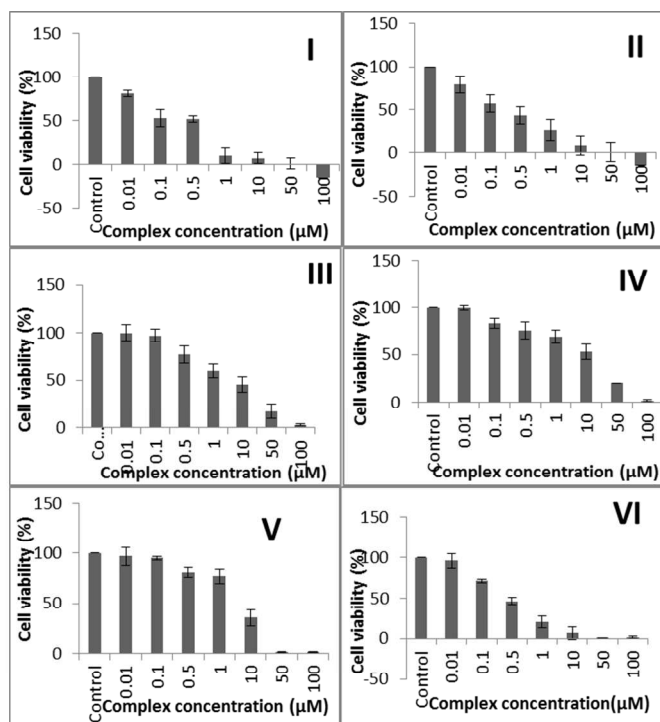


Fig.8 Cell viability of oxovanadium(IV) complexes **I–VIII** on AGS gastric cell line *in vitro*. Each data point is the mean standard error obtained from three independent experiments.



The results indicate that though the ligands show little activity (Fig.S13) all the eight oxovanadium(IV) complexes exhibit anticancer activity against AGS gastric cells in a time and dose dependent manner with increasing concentrations of the complexes. As shown in the Fig.8, most of the complexes induced cell death in more than 90% of population. Complexes **I** and **II** showed complete killing of AGS cells at 100µM concentration. In complexes **V** and **VI**, 98% killing of the cells were observed. Complexes **III** and **IV** showed more or less similar changes in the cells and complex **VIII** showed minimum cell death when compared to other complexes.

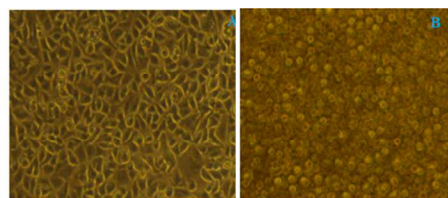


Fig. 9 Cell images A) before and B) after treatment with Complex **I** examined by fluorescence microscopy

The V(IV) complexes exhibit broad inhibition on the AGS gastric cell lines with IC₅₀ values ranging from 0.39 to 53.73. The IC₅₀ values of the complexes (Fig.S14 and Table S9 in the supporting information) suggest that complexes **I**, **II**, and **VI** possessed more

potent inhibitory effect against the cancer cells. Complex **IV** carrying -NO₂ group in the salphen ligand shows highest IC₅₀ value compelling us to propose that electronic effect may be one of the factors in determining the anti-cancer activities of V(IV)-salphen complexes.⁹⁰

Conclusion

In the present study, the protein binding properties of a series of salphen ligands and the oxovanadium(IV) complexes studied using different spectral methods support the interaction of oxovanadium(IV)-salphen complexes with BSA. The non-linear Stern-Volmer plots indicate that the quenching mechanism of BSA by oxovanadium(IV)-salphen complexes is by both static and dynamic processes. The shorter distance between tryptophan and probes calculated using Forster theory for the fluorescence quenching indicates more efficient energy transfer. The binding of oxovanadium(IV) complexes induced a conformational change of BSA evident from the CD spectra. The docking studies also reveal that there is a hydrophobic and hydrogen bonding interaction between the V(IV) complexes and BSA. These V(IV) complexes inhibit the growth of AGS gastric cell lines, which may provide the basis for the design of potentially effective target-specific drug for the treatment of cancer.

Acknowledgment

SR acknowledges UGC-BSR Faculty Fellow programme for financial support. RR acknowledges DST, New Delhi for financial support. VGS acknowledges UGC for the award of Faculty Development Programme. The authors thank Mr. R. Raghu for providing the Schrodinger software.

Notes and references

^aSchool of Chemistry, Madurai Kamaraj University, Madurai – 625 021, India. Fax: 91-452-2459139; Tel: 91-452-2458246; E-mail: rajagopalseenivasan@yahoo.com (S. Rajagopal)

^bSchool of Chemistry, Madurai Kamaraj University, Madurai – 625 021, India. Fax: 91-452-2459084; Tel: 91-452-2459181; E-mail: ramarajr@yahoo.com (R. Ramaraj)

^cCollege of Pharmacy, Madras Medical College, Chennai – 600003.

^dNRCBS, School of Biological Sciences, Madurai Kamaraj University, Madurai, 625 021, India.

^eSchool of Biological Sciences, Madurai Kamaraj University, Madurai, 625 021, India.

† Electronic Supplementary Information (ESI) available: [Detailed experimental, spectroscopic, computational, and further analytical details for the all vanadium complexes]. See DOI: 10.1039/b000000x/

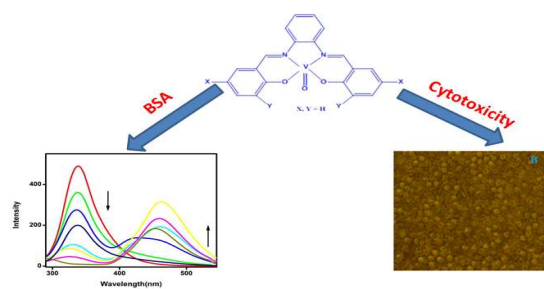
- 1 D. Rehder, *Bioinorganic Vanadium Chemistry*, John Wiley&Sons, New York, 2008.
- 2 S. M. Brichard and J. C. Henquin, *Trends in Pharmacol. Sci.*, 1995, **237**, 265–270.
- 3 I. Correia, J. Costa Pessoa, M. T. Duarte, R. T. Henriques, M. F. M. Piedade, L. F. Verios, T. Jackush, A. Dornyei, T. Kiss, M. M. C. A. Castro, C. F. G. C. Geraldés and F. Aveçilla, *Chem. Eur. J.*, 2004, **10**, 2301–2317.
- 4 H. Sakurai, Y. Kojima, Y. Yoshikawa, K. Kawabe and H. H. Yasui, *Coord. Chem. Rev.*, 2002, **226**, 187–198.
- 5 B. D. Liboiron, K. H. Thompson, G. R. Hanson, E. Lam, N. Aebischer and C. Orvig, *J. Am. Chem. Soc.*, 2005, **127**, 5104–5115.
- 6 T. Mukherjee, J. C. Pessoa, A. Kumar and A. R. Sarkar, *Inorg. Chem.*, 2011, **50**, 4349–4361.

- 7 T. Kiss, E. Kiss, E. Garriba and H. Sakurai, *J. Inorg. Biochem.*, 2000, **80**, 65–73.
- 8 F. Bosca, *J. Phys. Chem. B*, 2012, **116**, 3504–3511.
- 9 N. S. Venkataramanan, G. Kuppuraj and S. Rajagopal, *Coord. Chem. Rev.*, 2005, **249**, 1249–1268.
- 10 M. F. S. Teixeira, E. R. Dockal and E. T. G. Cavalheiro, *Sensors and Actuators B*, 2005, **106**, 619–625.
- 11 N. H. Campell, N. H. Abd Karim, G. N. Parkinson, M. Gunaratnam, V. Petrucci, A. K. Todd, R. Vilar and S. Neidle, *J. Med. Chem.*, 2012, **55**, 209–222.
- 12 M. A. Kamyabi and F. Aghajani, *J. Electroanal. Chem.*, 2008, **614**, 157–165.
- 13 M. P. Weberski Jr., C. C. McLauchlan and C. G. Hamaker, *Polyhedron*, 2006, **25**, 119–123.
- 14 Z. G. Yaseen, *J. Chem. Pharm. Research*, 2012, **4**, 3361–3367.
- 15 X. M. He and D. C. Carter, *Nature*, 1992, **358**, 209–215.
- 16 T. Banerjee, S. K. Singh and N. Kishore, *J. Phys. Chem. B*, 2006, **110**, 24147–24156.
- 17 D. Sanna, L. Biro, P. Buglyo, G. Micera and E. Garriba, *Metalomics*, 2012, **4**, 33–36.
- 18 A. L. Noffke, A. Habtemariam, A. M. Pizarro and P. J. Sadler, *Chem. Comm.*, 2012, **48**, 5219–5246.
- 19 M. Ping, Z. Li-Xia, L. Y. C. Li-Hua and H. Pei-Zhi, *Chin. J. Chem.*, 2008, **28**, 85–89.
- 20 N. Shahabadi and M. Maghasudi, *J. Mol. Str.*, 2009, **929**, 193–199.
- 21 J. S. Y. Lau, P. K. Lee, K. H. K. Tsang, C. H. C. Ng, Y. W. Lam, S. Cheng and K. K. W. Lo, *Inorg. Chem.*, 2009, **48**, 708–718.
- 22 K. Y. Zhang, S. P. Y. Li, N. Zhu, I. W. S. Or, M. S. H. Cheung, Y. W. Lam and K. K. W. Lo, *Inorg. Chem.*, 2010, **49**, 2530–2540.
- 23 K. K. W. Lo and K. Y. Zhang, *RSC Adv.*, 2012, **2**, 12069–12083.
- 24 V. Sathish, E. Babu, A. Ramdass, Z. Z. Lu, T. -T Chan, M. Velayudham, P. Thanasekaran, K. L. Lu, W. S. Li and S. Rajagopal, *RSC Adv.*, 2013, **3**, 18557–18566.
- 25 J. Bhuvanewari, A. K. Fathima and S. Rajagopal, *J. Photochem. Photobiol. A: Chem.*, 2012, **227**, 38–46.
- 26 J. Bhuvanewari, P. Muthu Mareeswaran, S. Shunmugasundaram and S. Rajagopal, *Inorg. Chim. Acta.*, 2011, **375**, 205–212.
- 27 P. Muthu Mareeswaran, D. Maheshwaran, E. Babu and S. Rajagopal, *J. Fluoresc.*, 2012, **22**, 1345–1356.
- 28 E. Babu, S. Singaravadiivel, P. Manojkumar, S. Krishnasamy, G. Gnana kumar and S. Rajagopal, *Anal. Bioanal. Chem.*, 2013, **405**, 6891–6895.
- 29 E. Babu, P. Muthu Mareeswaran and S. Rajagopal, *J. Fluoresc.*, 2012, **22**, 145–154.
- 30 F. G. Ferrer, A. Bosch, O. Yantorno and E. Baran, *J. Bioorg. Med. Chem.* 2008, **16**, 3878–3886.
- 31 P. K. Samsal, S. Saha, R. Majumdar, S. De, R. R. Dighi and A. R. Chakravarty, *Dalton Trans.* 2010, **39**, 2147–2158.
- 32 T. Hamada, M. Asanuma, T. Ueki, T. F. Hayashi, N. Kobayashi, S. Yokoyama, H. Michibata and H. Hirota, *J. Am. Chem. Soc.* 2005, **127**, 4216–4222.
- 33 J. R. Zamian, E. R. Dockal, G. Castellano and G. Olivo, *Polyhedron*, 1995, **14**, 2411–2418.
- 34 R. Sevvell, S. Rajagopal, C. Srinivasan, N. M. I. Alhaji and A. Chellamani, *J. Org. Chem.*, 2000, **65**, 3334–3340.
- 35 M. P. Weberski Jr., C. C. McLauchlan, C. G. Hamaker, *Polyhedron*, 2006, **25**, 119–123.
- 36 K. A. Majorek, P. J. Porebski, M. Chruszcz, M. D. Zimmerman, A. J. Stewart, A. Dayal, K. Jablonska and W. Minor, *Mol. Immunol.* 2012, **52**, 174–182.
- 37 A. T. Laurie and R. M. Jackson, *Bioinform.* 2005, **21**, 1908–1916.
- 38 D. E. Shaw, *J. Comp. Chem.* 2005, **26**, 1318–1328.
- 39 P. A. Greenidge, C. Kramer, J. C. Mozziconacci, and R. M. Wolf, *J. Chem. Inf. Model.* 2013, **53**, 201–209.
- 40 S. Denizot, R. Lange, *J. Immunol. Meth.* 1986, **89**, 271–277.
- 41 D. M. Boghaei, A. Bezaatpour and M. Behzad, *J. Coord. Chem.*, 2007, **60**, 973.
- 42 T. Alsalam, J. S. Hadi, E. A. Al-Nasir, H. S. Abbo and S. J. J. Titinchi, *J. Catal. Lett.*, 2010, **136**, 228–233.
- 43 M. Pasquali, F. Marchetti and C. Floriani, *J. Chem. Soc., Dalton Trans.* 1977, 139–144.

Dalton Transactions Accepted Manuscript

- 44 V. Berau, V. Jubera, P. Arnaud, A. Kaiba, P. Guionneaud and J. P. Sutter, *Dalton Trans.*, 2010, **39**, 2070–2077.
- 45 N. A. Lewis, F. Liu, L. Seymour, A. Magnusen, T. R. Erves, J. F. Arca, F. A. Beckford, R. Venkatraman, A. G. Sarrías, F. R. Fronczek, D. G. VanDerveer, N. P. Seeram, A. Liu, W. L. Jarrett and A. A. Holder, *Eur. J. Inorg. Chem.*, 2012, **4**, 664–677.
- 46 A. Sarkar and S. Pal, *Polyhedron*, 2006, **25**, 1689–1694.
- 47 S. Samanta, D. Ghosh, S. Mukhopadhyay, A. Endo, T. J. R. Weakley and M. Chaudhury, *Inorg. Chem.* 2003, **42**, 1508–1517.
- 48 E. Carter, I. A. Fallis, B. M. Kariuki, I. R. Morgan, T. Murphy, D. M. Tatchell, S. Van Doorslaer and E. Vinck, *Dalton Trans.* 2011, **40**, 7454–7462.
- 49 A. H. Kianfar and S. Mohebbi, *J. Iran. Chem. Soc.* 2007, **4**, 215–220.
- 50 A. Chellamani, P. Kulanthaipandi and S. Rajagopal, *J. Org. Chem.* 1999, **64**, 2232–2239.
- 51 V. K. Sivasubramanian, M. Ganesan, S. Rajagopal and R. Ramaraj, *J. Org. Chem.* 2002, **67**, 1506–1514.
- 52 N. S. Venkataramanan, S. Premsingh, S. Rajagopal and K. Pitchumani, *J. Org. Chem.* 2003, **68**, 7460–7470.
- 53 A. Mary Imelda Jayaseeli and S. Rajagopal, *J. Mol. Catal. A: Chem.*, 2009, **309**, 103–110.
- 54 S. Premsingh, N. S. Venkataramanan, S. P. Mirza, M. Vairamani, P. Sambasiva Rao, K. Velavan and S. Rajagopal, *Inorg. Chem.* 2004, **43**, 5744–5753.
- 55 M. Cametti, A. Dalla Cort and L. Mandolin, *Chem. Sci.*, 2012, **3**, 2119–2112.
- 56 A. Coletti, P. Galloni, A. Sartorel, V. Conte and B. Floris, *Catal. Today*, 2012, **192**, 44–55.
- 57 V. Conte, F. Fabbianesi, B. Floris, P. Galloni, D. Sordi, I. W. C. E. Arends, M. Bonchio, D. Rehder and D. Bogdal, *Pure Appl. Chem.*, 2009, **81**, 1265–1277.
- 58 S. Sarika, M. L. P. Reddy, A. H. Cowley and K. V. Vasudevan, *Dalton Trans.* 2010, **39**, 776–786.
- 59 A. A. Holder, P. Taylor, A. R. Magnusen, E. T. Moffett, K. Meyer, Y. Hong, S. E. Ramsdale, M. Gordon, J. Stubbs, L. A. Seymour, D. Acharya, R. T. Weber, P. F. Smith, G. C. Dismukes, P. Ji L. Menocal, F. Bai, J. L. Williams, D. M. Crokek and W. L. Jarrett, *Dalton Trans.*, 2013, **42**, 11881–99.
- 60 E. Carter, I. A. Fallis, D. M. Murphy, D. J. Willock, S. V. Doorslaer and E. Vinck, *Chem. Phys. Lett.* 2010, **486**, 74–79.
- 61 D. Sanna, G. Micera and E. Garribba, *Inorg. Chem.*, 2013, **52**, 11975–11985.
- 62 H.A. Benesi and J. H. Hildebrand, *J. Am. Chem. Soc.*, 1949, **71**, 2703–2707.
- 63 E. Gok, C. Ozturk and N. Akbay, *J. Fluoresc.*, 2008, **18**, 781–785.
- 64 J. R. Lakowicz, *Principles of Fluorescence Spectroscopy*, 3rd ed.; Kluwer Academic/Plenum Publishers: New York, 2006.
- 65 B. Manimaran, L.-J. Lai, P. Thanasekaran, J.-Y. Wu, R.-T. Liao, T.-W. Tseng, Y.-H. Liu, G.-H. Lee, S.-M. Peng and K.-L. Lu, *Inorg. Chem.*, 2006, **45**, 8070–8077.
- 66 B. Ojha and G. Das, *J. Phys. Chem. B*, 2010, **114**, 3979–3986.
- 67 S. S. Iqbal, M. W. Mayo, J. G. Bruno, B. V. Bronk, C. A. Batt and J. P. Chamber, *Biosen. Bioelect.* 2000, **15**, 549–578.
- 68 P. Banerjee, S. Pramanik, A. Sarkar and S. C. Bhattacharya, *J. Phys. Chem. B*, 2009, **113**, 11429–11436.
- 69 P. B. Kandagal, P. Asoka, J. Seetharamappa, S. M. T. Shaikh, Y. Jadegond and O. B. Ijare, *J. Pharm. Biomed. Anal.*, 2006, **41**, 393–399.
- 70 F. Samari, B. Hemmateenejad, M. Shamsipur, M. Rashidi and H. Samouei, *Inorg. Chem.*, 2012, **51**, 3454–3464.
- 71 B. Valeur and J. C. B. rochon, *New Trends in Fluorescence Spectroscopy*; Springer: Berlin, 2001, 25.
- 72 Z. Chi, R. Liu, Y. Teng, X. Fang and C. Gao, *J. Agric. Food Chem.* 2010, **58**, 10262–10269.
- 73 S. P. Upadhyay, R. R. S. Pissurlenkar, E. C. Coutinho and A. V. Karnik, *J. Org. Chem.*, 2007, **72**, 5709–5714.
- 74 N. Ibrahim, N. H. Ibrahim, S. Kim, J. P. Nallet and F. Nepveu, *Biomacromol.*, 2010, **11**, 3341–3351.
- 75 G. Zhang, Y. Wang, H. Zhang, S. Tang and W. Tao, *Pest. Biochem. Physiol.* 2007, **87**, 23–29.
- 76 B. Chakraborty, A. Singha Roy, S. Dasgupta and S. Basu, *J. Phys. Chem. A.*, 2010, **114**, 13313–13325.
- 77 N. C. Price, *Biotech. Applied Biochem.*, 2000, **31**, 29–40.
- 78 H. Gao, L. Lei, J. Liu, Q. Kong, X. Chen and Z. Hu, *J. Photochem. Photobiol. A: Chem.* 2004, **167**, 213–221.
- 79 W. Y. Qing, T. B. Ping, Z. H. Mei, Z. Q. Hu and Z. G. Cheng, *J. Photochem. Photobiol. B: Biol.*, 2009, **94**, 183–190.
- 80 S. C. Wang and C. T. Lee Jr, *J. Phys. Chem. B*, 2006, **110**, 16117–16123.
- 81 We thank one of the reviewers for bringing this point to our notice.
- 82 D. M. Murphy, I. A. Fallis, E. Carter, D. J. Willock, J. Landon, S. V. Doorslaer and E. Vinck, *Phys.Chem.Chem.Phys.*, 2009, **11**, 6757–6769.
- 83 R. Subramanyam, M. Goud, B. Sudhamalla, E. Reddeem, A. Gollapudi, S. Nellaepalli, V. Yadavalli, M. Chinnaboina and D. G. Amooru, *J. Photochem. Photobiol. B: Biol.* 2009, **95**, 81–88.
- 84 D. C. Carter and J. X. Ho, *Adv. Protein Chem.* 1994, **45**, 153–203.
- 85 L. Huang and T. Kim, *Biol. Med.* 2004, **37**, 735–736.
- 86 J. A. Hamilton, S. Era, S. P. Bhamidipati and R. G. Reed, *Proc. Natl. Acad. Sci. USA*. 1991, **88**, 2051–2054.
- 87 J. Yu, Y. Zhou, I. Tanaka and M. Yao, *Bioinformatics*, 2010, **26**, 46–52.
- 88 G. L. Francis, *Cytotechnology*, 2010, **62**, 1–16.
- 89 A. K. Haldar, P. Sen and S. Roy, *Mol. Biol. Inter.* 2011, 1–23.
- 90 Y. Zhang, X. Wang, W. Fang, X. Cai, F. Chu, X. Liao and J. Lu, *Bioinorg. Chem. Appl.* 2013, 1–14.

Table of Contents (TOC) figure



An oxovanadium(IV)-salphen complex acts as a probe for bovine serum albumin and shows cytotoxicity against cancer cells.